Upcycling industrial residues into tobermorite-bearing calcium silicate hydrates: structural, morphological, and surface characterization

Reciclagem de resíduo industrial em silicatos de cálcio hidratado contendo tobermorita: caracterização estrutural, morfológica e de superfície

Reciclaje de residuos industriales en silicatos de calcio hidratados conteniendo tobermorita: caracterización estructural, morfológica y superficial

DOI: 10.34188/bjaerv9n1-162

Submeted: Jan 5th, 2026
Approved: Feb 4 th, 2026

Raquel Reis Alcântara-Domingos
Master in Sciences in the area of concentration in Nuclear Technology in Materials at Nuclear Energy Research Institute (IPEN/CNEN). Brazil
São Paulo, SP. Brasil
E-mail: rreisa@hotmail.com

Danilo Lopes Costa e Silva
PhD in Sciences in the area of concentration in Nuclear Technology in Materials at Nuclear Energy Research Institute (IPEN/CNEN). Brazil
São Paulo, SP. Brasil
E-mail: dalocs@gmail.com

Igor Yamamoto Abê
Master in Electrical Engineering from the University of São Paulo. Brazil
São Paulo, SP. Brasil
E-mail: igor.abe@usp.br

Felipe Bonito Jaldin Ferrufino
Master in Sciences in the area of concentration in Nuclear Technology in Engineering at Nuclear Energy Research Institute (IPEN/CNEN). Brazil
São Paulo, SP. Brasil
E-mail: fbferr@gmail.com

Denise Alves Fungaro
PhD in Chemical at Energy Research Institute, University of Sao Paulo (IPEN/CNEN - USP). Brazil.
São Paulo, SP. Brasil
E-mail: dfungaro@ipen.br

ABSTRACT

Considering the increasing volume of industrial waste and the gaps in the literature regarding the integrated correlation between the crystalline structure, microstructure, and surface properties of hydrated calcium silicate compounds obtained exclusively from complex waste, this study addresses the valorization of FGD ash for the synthesis of tobermorite-containing materials. The objective was to integratively characterize a C–S–H compound previously synthesized from FGD, focusing on structural, morphological, and textural confirmation for environmental applications. The material

was characterized by XRF, XRD, FTIR, Raman, SEM/EDS, TGA, helium pycnometry, particle size distribution, and N_2 adsorption (BET/BJH), in addition to a brief bibliometric analysis for scientific contextualization. The results indicated a composition rich in SiO_2 (26.1%) and CaO (23.1%), with a Ca/Si ratio of ≈0.89 and significant presence of Na, Mg, and Al. XRD confirmed the formation of tobermorite associated with semicrystalline C–S–H compound phases. FTIR and Raman evidenced silicate chains Q^1–Q^3, while SEM revealed a typical lamellar morphology. The true density was 2.10 $g \cdot cm^{-3}$, and the specific surface area was 14.85 $m^2 \cdot g^{-1}$, with predominantly mesoporous porosity (≈21 nm). TGA demonstrated thermal stability up to ~450 °C. It is concluded that the adopted process enabled the production of a structurally stable and texturally suitable multiphasic material for environmental applications, contributing to circular economy strategies and the valorization of industrial waste.

Keywords: calcium silicate hydrate, FGD ash, tobermorite, multiple characterizations, industrial waste.

RESUMO

Considerando o crescente volume de resíduos industriais e as lacunas na literatura quanto à correlação integrada entre estrutura cristalina, microestrutura e propriedades de superfície de compostos de silicatos de cálcio hidratados obtidos exclusivamente de resíduos complexos, este estudo aborda a valorização de cinzas FGD para síntese de materiais contendo tobermorita. O objetivo foi caracterizar de forma integrada composto C–S–H sintetizado previamente a partir de FGD, com foco na confirmação estrutural, morfológica e textural, visando aplicações ambientais. O material foi caracterizado por XRF, DRX, FTIR, Raman, SEM/EDS, TGA, picnometria de hélio, distribuição granulométrica e adsorção de N_2 (BET/BJH), além de uma breve análise bibliométrica para contextualização científica. Os resultados indicaram composição rica em SiO_2 (26,1%) e CaO (23,1%), com razão Ca/Si ≈ 0,89 e presença significativa de Na, Mg e Al. O DRX confirmou a formação de tobermorita associada a fases de composto C–S–H semicristalinas. FTIR e Raman evidenciaram cadeias silicatadas Q^1–Q^3, enquanto SEM revelou morfologia lamelar típica. A densidade real foi 2,10 $g \cdot cm^{-3}$, e a área superficial específica foi 14,85 $m^2 \cdot g^{-1}$, com porosidade predominantemente mesoporosa (≈21 nm). A TGA demonstrou estabilidade térmica até ~450 °C. Conclui-se que o processo adotado permitiu obter material multifásico estruturalmente estável e texturalmente adequado para aplicações ambientais, contribuindo para estratégias de economia circular e valorização de resíduos industriais.

Palavras-chave: silicatos de cálcio hidratados, cinzas FGD, tobermorita, múltiplas caracterizações, resíduos industriais.

RESUMEN

Considerando el creciente volumen de residuos industriales y las lagunas en la literatura en cuanto a la correlación integrada entre la estructura cristalina, la microestructura y las propiedades superficiales de compuestos de silicatos de calcio hidratados obtenidos exclusivamente de residuos complejos, este estudio aborda la valorización de cenizas FGD para la síntesis de materiales que contienen tobermorita. El objetivo fue caracterizar de forma integrada un compuesto C–S–H previamente sintetizado a partir de FGD, con énfasis en la confirmación estructural, morfológica y textural, orientado a aplicaciones medioambientales. El material fue caracterizado mediante FRX, DRX, FTIR, Raman, SEM/EDS, TGA, picnometría de helio, distribución granulométrica y adsorción de N_2 (BET/BJH), además de un breve análisis bibliométrico para la contextualización científica. Los resultados indicaron una composición rica en SiO_2 (26,1%) y CaO (23,1%), con una relación Ca/Si ≈0,89 y presencia significativa de Na, Mg y Al. El DRX confirmó la formación de tobermorita asociada a fases semicristalinas del compuesto C–S–H. FTIR y Raman evidenciaron cadenas de silicatos Q^1–Q^3, mientras que el SEM reveló una morfología laminar típica. La densidad

real fue de 2,10 g·cm^{-3} y el área superficial específica de 14,85 m^2·g^{-1}, con una porosidad predominantemente mesoporosa (≈21 nm). La TGA demostró estabilidad térmica hasta ~450 °C. Se concluye que el proceso adoptado permitió obtener un material multifásico, estructuralmente estable y texturalmente adecuado para aplicaciones medioambientales, contribuyendo a estrategias de economía circular y valorización de residuos industriales.

Palabras clave: silicato de calcio hidratado, cenizas FGD, tobermorita, caracterizaciones múltiples, residuos industriales.

1 INTRODUCTION

The increasing generation of industrial waste, such as coal combustion ashes, steel slags, and construction and demolition waste, stands as an urgent socio-environmental challenge but also as a strategic opportunity for the circular economy, enabling the transformation of liabilities into valuable raw materials (Alsharari, 2025). The global rise of these residues and their disposal in landfills entail environmental risks and contamination, and propagate indirect CO_2 emissions, especially considering, for example, the high impacts associated with Portland cement production (Durastanti and Moretti, 2020). Additionally, alignment with the Sustainable Development Goals (SDGs), the energy transition, and green engineering reinforce the importance of rethinking industrial flows from a sustainable perspective (Ismail et al., 2025; Ferraz et al., 2023). In this context, the reuse of these wastes in high-value-added materials, such as alternative cementitious binders, represents a promising route for reducing the carbon footprint of construction and fostering more resilient production chains (Khalifa et al., 2020).

Calcium silicate hydrate (C–S–H) is the predominant phase resulting from the hydration of Portland cement, typically accounting for about 60–70% of the solid products and being primarily responsible for the mechanical strength of cementitious pastes (Li et al., 2024; Gartner et al., 2017; Taylor, 1997). Furthermore, C–S–H exhibits a highly porous microstructure with a high surface area, which gives it a remarkable capacity for adsorbing metallic ions and important mechanisms for the immobilization of heavy metals such as Cs, U, Pb, and Cr through ionic substitution and encapsulation within the interstitial network (LIU et al., 2023; ZHU et al., 2024; Zak and Deja, 2015). Moreover, studies show that synthetic forms of C–S–H, including those derived from wastes such as fly ash, can efficiently adsorb heavy metals through complexation, ion exchange, and electrostatic interactions, combining high performance with low cost and impact (Sun et al., 2022). These findings reinforce the growing interest in synthesizing C–S–H from alternative calcium and silica sources, not only to reduce the use of cement clinker, which is responsible for high CO_2 emissions, but also to develop functional materials.

There are different types of C–S–H compounds, among which tobermorite stands out.

Tobermorite is a particularly stable crystalline phase in the C–S–H system, essential for advanced applications, as this mineral structure has dense silicate chains and a lamellar organization that gives it high thermal stability, already demonstrated by controlled transformations at temperatures up to ~150 °C (Galvánková et al., 2016; Richardson, 2008). Its well-defined porosity and interlayer structure allow for effective ion exchange, with the capacity to adsorb heavy metal cations via substitution at calcium sites, making it ideal as an adsorbent or confinement matrix (HURT et al., 2022). Moreover, tobermorite exhibits high mechanical strength and structural integrity, especially when doped (for example, with Mg, Sr, or Ba), improving elastic moduli and durability (LI et al., 2020). These characteristics make tobermorite a versatile material, with applications not only in cementitious binders, such as in autoclaved concrete, but also in adsorbents for remediation, ion exchangers in waste treatment, and even in catalysts, exploiting its robustness and chemical selectivity (Rahman et al., 2022).

Flue Gas Desulfurization ash (FGD), resulting from coal combustion, represents a significant environmental challenge. These ashes are rich in oxides such as CaO, SiO_2, S, and alkaline elements, and their improper disposal can lead to soil and water contamination, as well as contributing to greenhouse gas emissions (Milak et al., 2025).

On the other hand, FGD ash has proven to be a promising precursor for the synthesis of C–S–H compounds containing tobermorite, precisely because it is a low-cost source of silica and calcium. The synthesized C–S–H compounds, specifically tobermorite and Al-tobermorite, were successfully obtained and showed high, selective adsorption capacity for Cs+ ions (Lalhmunsiama et al., 2021; Fungaro et al., 2020).

Another residue, such as blast furnace slag, has been used to prepare tobermorite via hydrothermal reaction, demonstrating the feasibility of utilizing wastes with different chemical compositions for obtaining C–S–H compounds (Rodriguez et al., 2026).

The use of wastes (fly ash, slag, mining residues, or glass) presents significant technical obstacles, including chemical heterogeneity among batches, the presence of impurities (trace metals, variable alumina, sulfates), and crystallinity (Alcântara-Domingos and Fungaro, 2025).

There is a variety of synthesis routes applied to obtaining C–S–H and tobermorite from wastes, among which hydrothermal/autoclave treatment, alkaline fusion followed by hydration, direct alkaline activation of powders (assisted geopolymerization), and mechanical and caustic pretreatment strategies (milling, NaOH) stand out, to increase the solubilization of silica and calcium from the precursors (Malferrari, 2025; Quan, 2025).

Studies converge that critical parameters, particularly the Ca/Si molar ratio, temperature and reaction time, pH/caustic strength (presence of NaOH/KOH), water/solid ratio, and the use of

additives or crystalline seeds govern the dissolution kinetics and the crystallization of tobermorite. For example, a low Ca/Si favors phases rich in gelatinous silicate, while Ca/Si ≈ 0.8–1.5 and moderate hydrothermal temperatures (120–220 °C) tend to favor the formation of more crystalline tobermorite (Malferrari et al., 2022).

Recurring limitations in the synthesized products are low crystallinity, the concurrent formation of secondary phases (for example, C–A–S–H gel, katoite, hydroxides) when the residue composition is complex, and the difficulty of obtaining pure tobermorite without purification steps (Yang et al., 2023).

In addition to the different synthesis methods for C–S–H compounds, detailed characterization of the obtained products is necessary to confirm their structural, morphological, and surface properties.

Fungaro et al. (2020) synthesized C–S–H compounds from FGD wastes and confirmed the presence of tobermorite through XRD, XRF, and SEM. Chen et al. (2022) FGD gypsum–based compounds were synthesized via a hydrothermal method and morphologically characterized by electron microscopy, with a detailed analysis of the morphology and dimensions of the fibers formed. Siauciunas et al. (2021) investigated the porosity of C–S–H synthesized from natural rocks, using BET and SEM. Madadi and Wei (2022) characterized C–S–H gels with different Ca/Si ratios by FTIR, Raman, XRD, and TGA. These works show that a multi-technical approach is essential for a comprehensive understanding of the properties of synthesized C–S–H compounds.

Bibliometric analysis has been widely employed as a robust tool to map the evolution of knowledge, identify emerging trends, thematic relationships, and scientific gaps in complex and interdisciplinary areas. These approaches allow a systematic and quantitative view of scientific production, complementing narrative analyses and reducing biases associated with subjective literature selection (Donthu et al., 2021; Aria and Cuccurullo, 2017). In this context, bibliometric visualization tools are used to analyze large sets of bibliographic data, enabling the construction of keyword co-occurrence maps, scientific collaboration networks, and dominant thematic structures in established and emerging research fields.

According to Van Eck and Waltman (2010), such maps make it possible to identify central conceptuais cores and their interconnections, providing relevant support for understanding scientific dynamics and the future direction of research. Applied to the area of alternative cementitious materials, bibliometric analysis has proved particularly effective in revealing the transition from the traditional focus on mechanical properties and structural performance to more integrated approaches that incorporate sustainability, industrial waste valorization, and environmental applications (Habert et al., 2020; Provis, 2018).

In the specific case of C–S–H compounds and tobermorite, this approach allows us to understand how different synthesis routes, characterization techniques, and applications have evolved and become interrelated over time.

Despite recent advances, the literature still shows a critical gap in the integrated understanding of the synthesis of C–S–H and tobermorite obtained exclusively from complex industrial residues. Although fly ashes, slags, and demolition wastes have been used as precursors, few studies systematically address sulfur-rich residues, such as FGD ashes, under controlled conditions of temperature, Ca/Si ratio, and solution mineralization (LI et al., 2022; Telesca et al., 2013).

Additionally, studies highlight that almost no research establishes direct correlations between synthesis parameters (pH, hydrothermal aging, aluminosilicate additives, and autoclave atmosphere) and the evolution of structural order, lamellar morphology, or specific surface area of the formed tobermorites (Quan et al., 2025; Yang et al., 2023; GROSCHE et al., 2018).

Most works focus only on the identification of the crystalline phase, neglecting integrated analyses involving XRD, FTIR, Raman, SEM/EDS, and BET, which limits the understanding of the effects of residue impurities (SO_4^{2-}, Al^{3+}, Mg^{2+}, Fe^{3+}) on phase purity, crystallinity, and the formation of undesirable secondary phases such as jennite or residual portlandite (Quan et al., 2025; Zhao et al., 2017; Vidmer et al., 2014). Thus, the literature lacks studies that combine synthesis from complex residues, in-depth structural characterization, and complete textural evaluation, highlighting the urgent need for approaches that clarify how sulfonated residues with high compositional variability influence the formation and stability of C–S–H compounds containing tobermorite.

The synthesis of C–S–H compounds with the presence of tobermorite from FGD was carried out using the alkaline fusion method followed by hydrothermal treatment with different synthesis parameters. The synthesized products consisted of semi-amorphous calcium silicate hydrate and tobermorite. The synthesis parameters were optimized to obtain the C–S–H compound with the highest relative intensity of the main tobermorite peak (Alcântara-Domingos and Fungaro, 2025). Therefore, the objective of the present work was to characterize these optimized synthetic C–S–H with detailed analysis focusing on confirming the structural, morphological, and surface properties, aiming to provide information about their potential for environmental applications.

2 METODOLOGIA

2.1 BIBLIOMETRY ANALYSIS

The collection of bibliographic data was carried out using the Scopus database. The search

strategy was structured based on a combination of terms related to the study theme, including keywords such as: calcium silicate hydrate, C-S-H, tobermorite, industrial waste, FGD, desulfurization ash, waste-derived, characterization, and characterization technique. The time period analyzed included all available publications from 2020 to 2025. Filters were applied to select documents of the article and review article types, published in peer-reviewed journals. After the initial extraction, the data underwent a pre-processing stage, including the removal of duplicates, standardization of equivalent terms, and exclusion of generic keywords without direct scientific relevance to the scope of the study. The processed bibliographic data were imported into VOSviewer software (version 1.6.20.0). The analysis was conducted through the construction of keyword co-occurrence maps, adopting the full counting method, in which all occurrences of a term are considered with the same weight. This method is recommended when seeking to comprehensively identify the conceptual structure of a research field (Van Eck and Waltman, 2010).

2.2 MATERIAL

All reagents used were of analytical grade, and the solutions were prepared with deionized water. The ashes from the flue gas desulfurization (FGD) system were collected from the thermoelectric power plant located in Candiota, Rio Grande do Sul, Brazil. Sodium hydroxide (NaOH) micropearls from Merck (P.A. 99%) were used for the synthesis of C-S-H compounds. Oven (Fanem Orion 515), mechanical stirrer equipped with a rod and paddle-type propeller, and muffle furnace (Quimis - model Q-318M24) were used. The characterization of the FGD ashes was published in a previous work (Alcântara-Domingos and Fungaro, 2025).

2.3 SYNTHESIS OF C-S-H COMPOUND

Synthesis of the C-S-H compound The C-S-H compound was synthesized from FGD by a two-step method under optimized conditions, following the methodology described in previous work (Alcântara-Domingos and Fungaro, 2025). Briefly, FGD: NaOH 1:1.2 (w/w) was mixed and heated to 600 °C for 1 h. The fused solid was ground, mixed with 200 mL of deionized water, agitated for 6 h and further hydrothermally treated at 100 °C for 24 h. Finally, the suspension was filtered and the solid was dried at 80 °C overnight. The sample was labeled SCF.

2.4 CHARACTERIZATION OF THE MATERIAL

Characterization of the material The chemical composition of the SCF compound was determined by X-ray fluorescence (XRF) using a Rigaku – RIX 3000 instrument. The mineralogical composition was determined by X-ray diffraction (XRD) with an automated Rigaku Multiflex

diffractometer with a copper anode, using Cu Kα radiation at 40 kV and 20 mA, in the (2θ) range of 5–60° with a scanning speed of 0.5°/min. The phases were identified by comparison with the PDF-2 database from the ICDD (International Centre for Diffraction Data). The specific mass of the material was determined by helium pycnometry, using a Micromeritics AccuPyc 1330 automatic pycnometer. Each measurement was performed in triplicate, and the mean value, expressed in $g \cdot cm^{-3}$, was calculated based on the volumetric variation of the inert gas. This technique allowed the estimation of the true density of the solid and inference of the presence of intraparticle porosity and the degree of structural compaction of the material. The particle size distribution was determined by laser diffraction using a particle size analyzer (Malvern/Mastersizer 2000). The particle size range (0–1000 µm) was evaluated based on cumulative volume, and the results were expressed as percentage distribution and mean diameter (D50). The Fourier transform infrared (FTIR) spectrum was obtained using a spectrometer (Nexus 670 Thermo Nicolet) in the range of 4000 to 400 cm^{-1}, with a resolution of 4 cm^{-1} and 32 scans. The sample was prepared in the form of a KBr pellet (1% w/w). The Raman spectrum was obtained using a WITEC Confocal Raman Microscope Alpha 300R, operating with a green Ar+ laser (532 nm), power of 45 mW, objective lens with 50x0.7 magnification, and integration time of 60 s. The powder sample was analyzed directly on an aluminum sample holder. The obtained spectrum was deconvoluted using Fityk software with Gaussian functions. Morphological analysis was carried out using a scanning electron microscope (SEM) (FEI-Current Thermo/Zeiss - QUANTA FEG 650/LEO 440). The sample was previously dried and coated with a carbon layer by vacuum metallization. The elemental composition was determined by energy dispersive spectroscopy (EDS), coupled to the SEM, with acquisition at multiple points on the surface. Thermal stability was evaluated by TGA analysis using a Mettler-Toledo instrument, under a nitrogen atmosphere, with a heating rate of 10 °C min^{-1} in the temperature range of 30 °C to 1000 °C. The derivative of the mass loss curve was used to identify decomposition and dehydration events of the present phases. The specific surface area and pore distribution were determined by N_2 adsorption at 77 K, using an automatic analyzer (ASAP 2020 Plus 1.03). The BET area was calculated from the linear range of the adsorption isotherm, and the pore size distribution was obtained by the BJH (Barrett–Joyner–Halenda) method.

3 RESULTS AND DISCUSSION

3.1 BIBLIOMETRY STUDY

The network map (Figure 1) reveals the formation of well-defined clusters, indicating that the research field is organized around central scientific axes. The terms microstructure, compressive strength, and tobermorite stand out, acting as high-centrality nodes that connect different lines of investigation.

Figure 1. Bibliometric network of keyword co-occurrence

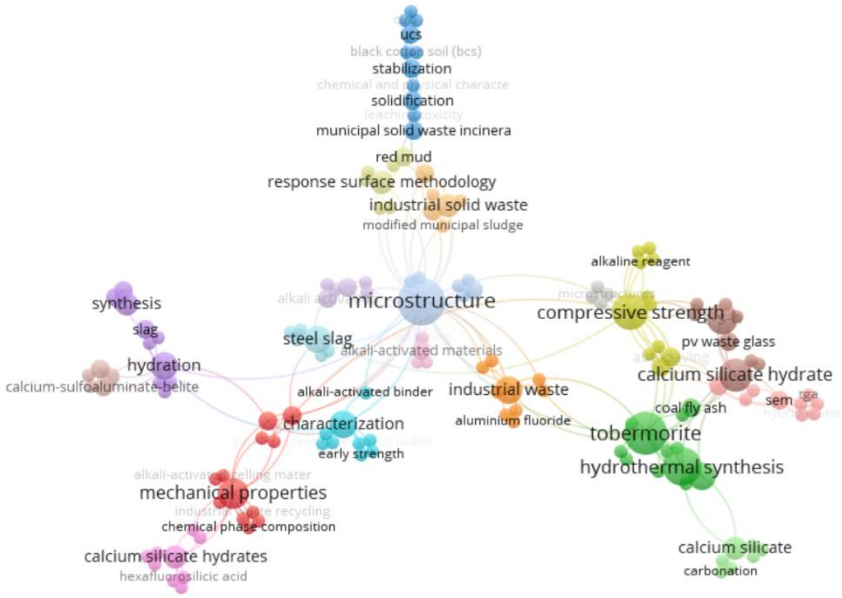

Source: Prepared by the authors

The term microstructure presents the highest centrality in the network, with strong connections to characterization, mechanical properties, alkali-activated binder, steel slag, ladle slag, and industrial solid waste. This configuration confirms that microstructure is widely recognized as the main link between composition, processing, and performance of cementitious materials and hydrated silicates derived from industrial waste (Scrivener et al., 2018). Associated with this core, there is a cluster related to mechanical properties and phase characterization, in which terms such as compressive strength, early strength, chemical phase composition, and calcium silicate hydrates appear strongly interconnected. This pattern reflects the classic approach in the literature, where mechanical strength is directly correlated with the formation, morphology, and structural evolution of C–S–H compound phases.

A second relevant thematic axis is defined by the cluster centered on tobermorite and hydrothermal synthesis, which is strongly connected to calcium silicate hydrate, coal fly ash, carbonation, and SEM. This organization demonstrates that the hydrothermal synthesis of tobermorite from silica- and calcium-rich wastes, especially coal fly ash, constitutes a consolidated and expanding line of research (Matsui et al., 2011; Zhang et al., 2020). The recurrence of the term coal fly ash reinforces the strategic role of this residue as an alternative raw material for the production of advanced hydrated silicates.

The map also shows consistent connections among industrial waste, industrial solid waste, recycled concrete powder, municipal solid waste incineration, and red mud, indicating a clear trend in the literature towards exploring valorization routes for industrial and urban wastes. These terms are connected to both the microstructure and mechanical strength clusters, suggesting that structural

performance remains a central criterion for the application of these materials. This trend aligns with works that highlight the conversion of waste into alternative cementitious materials as a key strategy for the circular economy and for reducing emissions associated with the construction industry (Wang et al., 2022; Habert et al., 2020).

The temporal visualization (Figure 2) shows a clear evolution of scientific focus over time. Terms such as hydration, slag, FGD gypsum, and pozzolans predominate in earlier periods, indicating that initial studies focused on the basic mechanisms of hydration and reactivity of alternative cementitious systems.

Figure 2. Temporal evolution

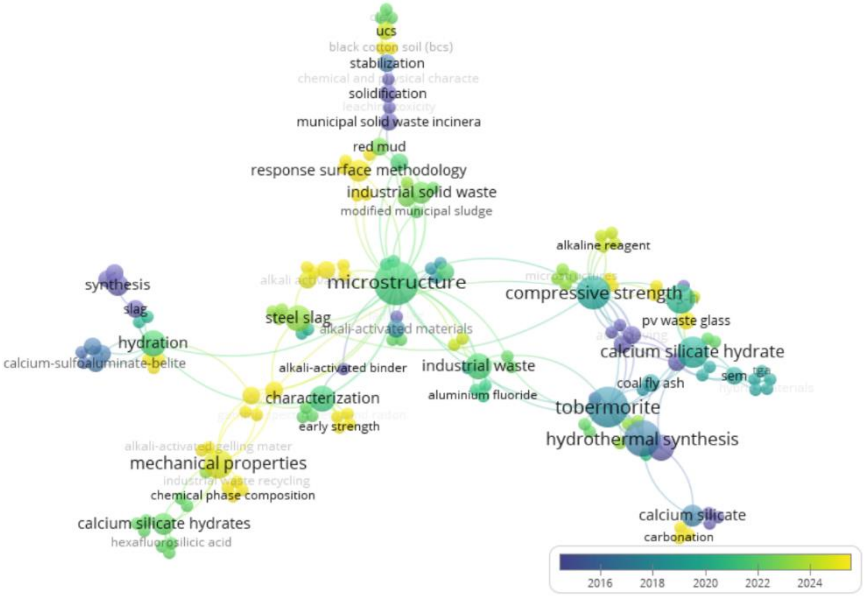

Source: Prepared by the authors

In contrast, more recent keywords such as tobermorite, hydrothermal synthesis, industrial waste valorization, alkali reagent, and response surface methodology appear associated with more recent periods, reflecting the field's advancement towards more sophisticated approaches involving optimization of synthesis parameters, microstructural control, and the development of functional materials with applications beyond conventional construction. This temporal shift indicates a transition from a predominantly mechanical focus to a more integrated approach, considering structure, process, performance, and sustainability (Lothenbach et al., 2011; Provis, 2020).

Despite the maturity observed in different areas, the bibliometric analysis reveals significant gaps. Although tobermorite and calcium silicate hydrate are widely investigated, there is still a lack of studies that systematically correlate the crystalline structure, microstructure, and surface properties of hydrated silicates synthesized from industrial residues, especially when aimed at environmental applications.

In this context, the present study takes a strategic position by integrating the synthesis of calcium silicate hydrates containing tobermorite from industrial wastes with an integrated structural and functional characterization approach, helping to fill gaps identified both in the experimental literature and in the bibliometric analysis.

3.2 CHARACTERIZATION TECHNIQUES

3.2.1 XRF

Table 1 presents the chemical composition of the synthesized material (SCF) determined by XRF.

Table 1. Chemical composition (in % by mass) of the SCF compound synthesized from FGD ash

COMPONENTS	(% by MASS)	COMPONENTS	(% by MASS)
SiO_2	26.1	SO_3	0.61
CaO	23.1	K_2O	0.07
MgO	12.8	SrO_2	0.02
Na_2O	8.21	MnO	0.02
Al_2O_3	6.53	P_2O_5	0.02
Fe_2O_3	1.97	Cl	0.01
TiO_2	0.32	ZnO	< 0.01

Source: Prepared by the authors

The analysis revealed predominant levels of SiO_2 (26.1%) and CaO (23.1%), values that indicate a balance between calcium and silica, a condition favorable for the formation of calcium silicate hydrates, especially tobermorite and C–S–H phases (Khalili et al., 2025). In addition, the significant presence of MgO (12.8%) and Al_2O_3 (6.53%) suggests that part of the structure may be modified by the incorporation of magnesium and aluminum, leading to the formation of C–M–S–H or C–A–S–H phases, as described by Madadi and collaborators (2022).

The Na_2O content (8.21%) is noteworthy, as it is considerably higher than that reported in C–S–H obtained by conventional routes. Recent studies indicate that sodium can act both as an alkalizing agent in the synthesis process and be incorporated into interlayers or the silicate network, modifying the effective Ca/Si ratio and influencing the stability and adsorption properties of the material (Yang et al., 2023; Tsvetkov et al., 2020). This result is consistent with the findings of Fungaro et al. (2020), who observed sodium enrichment in C–S–H compounds synthesized from FGD ash, resulting from the original composition of the residue.

FGD ash not only supplies adequate CaO and SiO_2 as precursors for forming calcium silicate hydrate phases, but also contains different proportions of alkali oxides (e.g., K_2O) and other impurities that distinguish it from natural rocks or engineered precursors. For example, Milak et al.

(2025) reported a FGD residue with ~38 wt.% CaO and ~19 wt.% SiO_2, alongside minor alkali contents, highlighting that these compositional differences can influence both phase evolution and functional properties.

The Fe_2O_3 content (1.97%), although secondary, is consistent with the presence of an accessory phase observed by XRD, such as magnetite. Even in small quantities, this oxide can modify the color, thermal stability, and adsorption potential of the material (Yang et al., 2023).

In summary, the XRF results indicate that the sample presents a typical composition of C–S–H materials obtained from industrial residues, with Ca/Si ratios (~0.89) compatible with crystallized tobermorite, but with a notable high sodium content, which distinguishes this material from conventional compositions and may act both as a beneficial factor (in cation mobility) and as a challenge (in structural stability) (Madadi et al., 2022; Fungaro et al., 2020).

3.2.2 Specific mass

The specific mass determined by helium pycnometry for the analyzed sample was 2.10 g/cm³, with a standard deviation of 0.009 g/cm³. This value is lower than expected for pure crystalline phases such as tobermorite (2.45–2.60 g/cm³) or quartz (2.65 g/cm³), but is compatible with values for predominantly amorphous or semicrystalline calcium silicate hydrates. In recent studies, density values for C–S–H gels range from 1.9 to 2.3 g/cm³, depending on the Ca/Si ratio, the degree of silicate chain polymerization, and the presence of intraparticle porosity (LIU et al., 2025; SIAUCIUNAS et al., 2021). Thus, the result suggests the presence of a significant fraction of amorphous or poorly crystallized hydrated phases, which is consistent with the synthesis from FGD ash.

Furthermore, the difference between the obtained value (2.10 g/cm³) and that specified for dense materials (≈2.70 g/cm³) indicates that the solid contains a high fraction of porosity accessible to the pycnometer gas, reinforcing the importance of complementing the analysis with BET and SEM/EDS to characterize the porous structure. Similar values of reduced density have also been reported in C–S–H compounds obtained from industrial residues, such as slags and FGD gypsum, in which the incorporation of foreign ions (Na, Al, Mg) contributes to reducing network densification (CHEN et al., 2022).

3.2.3 Particle size analysis

The particle size distribution (Figure 3) showed particles ranging from <1 µm to >1000 µm, with the highest volume concentration between approximately 10 and 200 µm. The cumulative curve indicates that most of the solid fraction is below ~500 µm, with a smaller proportion of fine

particles.

Figure 3. Particle size distribution of the SCF compound obtained from FGD ash

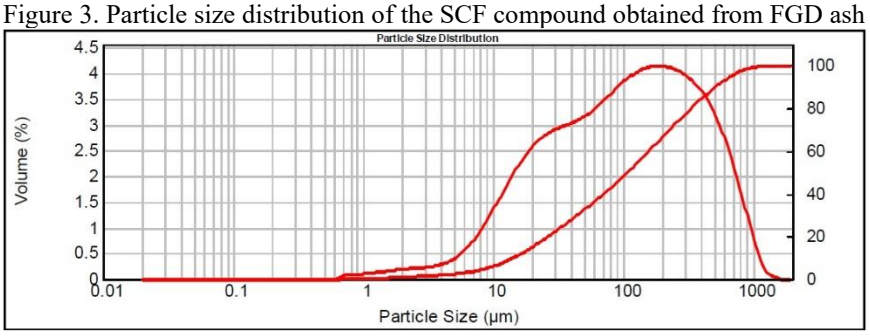

Source: Prepared by the authors

This behavior is typical of powders obtained by grinding FGD ash and reaction products from hydrothermal synthesis, which exhibit polydisperse and non-homogeneous distributions. Similar distributions are observed for materials derived from FGD gypsum, in which particles predominantly range between 5–100 µm, but with tails extending toward larger sizes due to the agglomeration of fine particles (LI et al., 2022). For C–S–H compounds synthesized from natural rocks and industrial residues, particle size ranges of 1–50 µm are commonly reported, but with a strong tendency toward aggregation into aggregates >100 µm, especially in materials rich in sodium or magnesium (Tang et al., 2021).

The predominance of micrometric particles, together with the presence of larger agglomerates, can impact properties such as surface area, reactivity, and adsorption capacity. Finer particles tend to increase reactivity and specific surface area, while larger agglomerates can reduce the homogeneity of the material (Malferrari et al., 2022; Siauciunas et al., 2021). Therefore, the heterogeneity observed in the particle size distribution reinforces the need for BET analysis to evaluate the fraction effectively available for interaction with contaminants.

The results obtained for specific mass and particle size distribution confirm that the SCF compound synthesized from FGD ash exhibits characteristics typical of partially amorphous C–S–H compounds, with lower density than pure crystalline phases and a polydisperse granulometry.

3.2.4 XRD

Figure 4 shows the diffractogram of the optimized sample (fusion time of 1 h, water volume of 200 mL, and agitation for 6 h), and Table 2 describes the crystallographic standards considered for result interpretation.

Figure 4. XRD of the SCF compound obtained from FGD ash

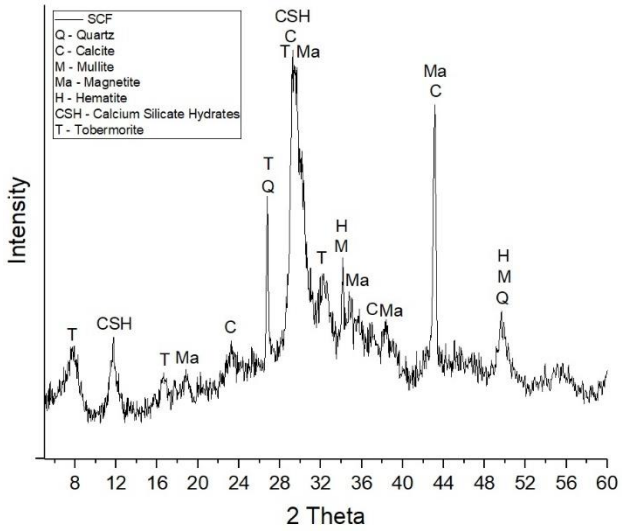

Source: Prepared by the authors

Table 2. XRD standards and chemical formulas of the main crystalline phases found in the FGD ash and SCF samples

PHASE	FORMULA	ICDD
Quartz	α-SiO_2	85-0796
Mullite	$3Al_2O_3.2SiO_2$	74-4143
Magnetite	Fe_3O_4	89-0691
Hematite	Fe_2O_3	89-0598
Calcite	$CaCO_3$	83-0578
Tobermorite	$Ca_5Si_6O_{16}(OH)_2 \cdot 4H_2O$	19-1364

Source: JCPDS-International Centre for Diffraction Data

A characteristic peak of tobermorite is observed around $2\theta \approx 8°$, associated with a basal spacing of 11 Å, accompanied by additional peaks at ~29° and ~49°, which are also consistent with the crystallographic standards of this phase (ICDD/JCPDS 19-1364). These results confirm the formation of tobermorite, as described in the literature (Diamond et al., 1963; Biagioni et al., 2015).

Additionally, broad and low-intensity peaks are noted in the region between 28–34°, attributed to semicrystalline C–S–H phases, in agreement with Maddalena et al. (2019). This behavior is typical of products from low-temperature hydrothermal synthesis, in which well-crystallized phases (tobermorite) coexist with partially amorphous phases (C–S–H).

Secondary phases were also identified, originating from the original composition of the FGD ash, such as quartz (~27°), calcite (~29° and 47°), magnetite (~36° and 44°), hematite (~33° and 54°), and mullite (~33° and 50°). The presence of these phases has likewise been reported in studies on desulfurization ashes (Grosch et al., 2018; XU et al., 2017).

Thus, the XRD analysis proves the successful synthesis of tobermorite and highlights the multiphase nature of the obtained material, providing essential support for integrated interpretation with other characterization techniques (FTIR, Raman, TGA, and SEM/EDS).

3.2.5 FTIR

Figure 5 presents the Fourier Transform Infrared (FTIR) spectrum of the material synthesized from FGD ash.

Figure 5. FTIR spectrum of the SCF compound obtained from FGD ash

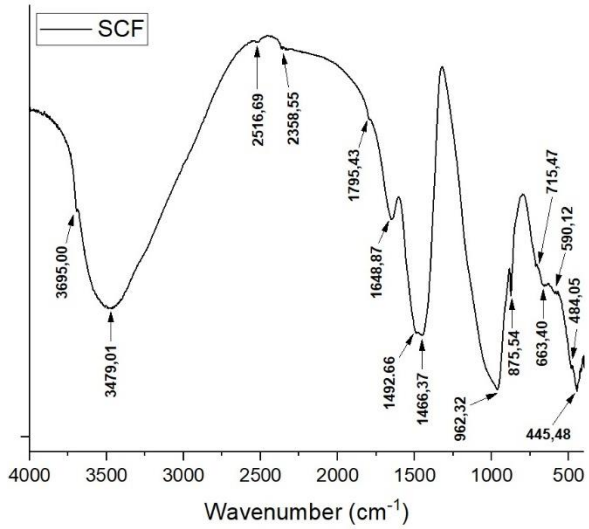

Source: Prepared by the authors

In the region of 3695–3479 cm^{-1}, a broad band can be observed, attributed to the O–H stretching of structural hydroxyl groups and adsorbed water molecules in the compound (Vidmer et al., 2014). The band at 1648 cm^{-1} is characteristic of the H–O–H bending of interlayer water present in C–S–H and tobermorite (Zhang et al., 2015; Kirkpatrick et al., 1997). In the region of 992 cm^{-1}, there is an intense band attributed to the asymmetric stretching of Si–O–Si bonds in the silicate chains, typical of calcium silicate hydrates. Similar results were reported by GUO et al. (2017), who also observed this band as indicative of tobermorite formation in hydrothermal synthesis. The bands at 875 and 715 cm^{-1} correspond to carbonate vibrations, related to the presence of residual calcite from the ashes, which is consistent with the XRD results and previous studies on FGD residues (Grosch et al., 2018; Kirkpatrick et al., 1997). In the region of 663–445 cm^{-1}, the bands can be associated with Si–O and Ca–O bond vibrations, characteristic of C–S–H phases. The presence of these bands confirms the formation of a silicate structure typical of hydrated cementitious materials (Maddalena et al., 2019). Overall, the FTIR results corroborate the synthesis of calcium silicate hydrates containing tobermorite, reinforcing the evidence obtained by XRD.

3.2.6 RAMAN

The Raman spectroscopy of the SCF compound presents a spectrum characteristic of C–S–H phases, with bands attributed to the different forms of silicon coordination (Q^n) in the silicate

chains. The specific meaning of the Q^n nomenclature can be explained as follows: n is the number of bridging oxygens, Q^0 represents an isolated Si–O tetrahedron (island), Q^1 represents a Si–O dimer tetrahedron, Q^2 represents a chain or ring Si–O tetrahedron, and Q^3 represents a sheet Si–O tetrahedron (Lothenbach et al., 2022; Kirkpatrick et al., 1997). Figure 6 shows the Raman spectrum of the SCF compound.

Nine main bands were identified, compatible with the presence of hydrated calcium silicate phases and accessory constituents (Kirkpatrick et al., 1997). Band 1 (~464 cm^{-1}) is attributed to the ν_2 (SiO_4) mode and the possible contribution of residual quartz, common in coal ash (Ortaboy et al., 2017). Band 2 (~540 cm^{-1}) is related to asymmetric deformations of Si–O–Si units and, in part, to sulfate modes, given the sulfate origin of the ash used (Ritz, 2023). Band 3 (~593 cm^{-1}) may be associated with the presence of hematite (α-Fe_2O_3), whose characteristic Raman signature occurs in this region, consistent with the Fe_2O_3 content identified in the sample (Jubb and Allen, 2010).

Figure 6. Raman spectra of the SCF compound synthesized from FGD ash where: [1] ν_2 mode; [2] Si–O–Si bending; [3] hematite (α-Fe_2O_3); [4] and [5] Q^2 vibrations; [6] Si–O in Q^1; [7] ν_1 mode (SO_4^{2-}); [8] Si–O stretching (Q^3–Q^4); and [9] – ν(OH) stretching

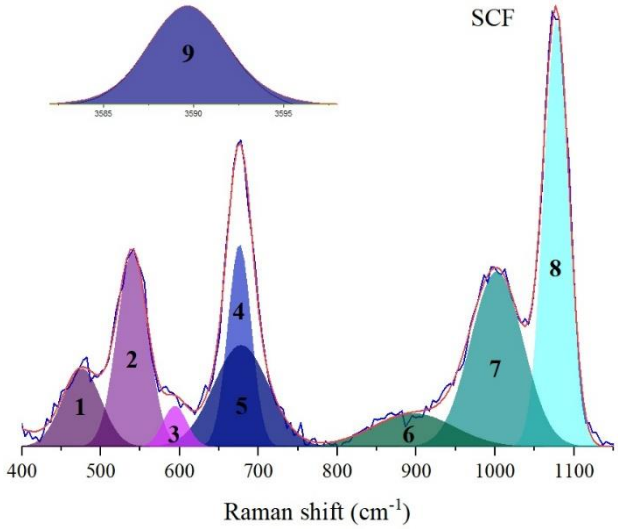

Source: Prepared by the authors

Band 4 (~675 cm^{-1}) represents the Q^2-Si–O–Si vibration, considered the main structural signature of tobermorite and C–S–H gels, being sensitive to the partial substitution of Si by Al in the chain (Ortaboy et al., 2017; Lothenbach et al., 2022). Band 5 (~677 cm^{-1}) corresponds to a subdivision of the previous one, related to different chain lengths and the presence of hydroxyls associated with calcium (Ortaboy et al., 2017; Kirkpatrick et al., 1997).

In the intermediate region, band 6 (~896 cm^{-1}) indicates the presence of poorly polymerized Q^1 units, compatible with calcium-rich C–S–H gels (Yan et al., 2018). Band 7 (~1001 cm^{-1}) can be attributed both to the ν_1 mode (SO_4^{2-}) of gypsum/anhydrite, corroborating the presence of sulfur in

the FGD ash, and to Si–O modes of Q^2/Q^3 units in partially polymerized chains (Ritz, 2023; Ortaboy et al., 2017). Band 8 (~1077 cm^{-1}) is related to the asymmetric stretching of the Si–O group in more polymerized units (Q^3–Q^4) and may also reflect the presence of secondary carbonates ($CaCO_3$), frequently formed by carbonation of C–S–H (Yan et al., 2022). Finally, band 9 (~3589 cm^{-1}) corresponds to the ν(OH) stretching of interlayer structural water or OH groups bound to Ca, indicating partial hydration and the presence of weakly bound water molecules (Jackson et al., 2017; Kirkpatrick et al., 1997).

The substitution of Si by Al in the network tends to shift and narrow the 670 cm^{-1} band, increasing structural order and cation exchange capacity (Lothenbach et al., 2022). The presence of Na from the residual matrix influences the polymerization of the silicate chain and may favor the stabilization of C–A–S–H-type species or even the partial formation of alkali-silicate phases (Yan et al., 2022). Thus, the obtained spectrum confirms the coexistence of typical tobermorite/C–S–H phases with contributions from sulfate, carbonate, and iron oxides, consistent with the complex nature of the sulfate ash precursor.

3.2.7 SEM/EDS

The images obtained from the morphological and elemental characterization of the synthesized SCF material are shown in Figure 7.

The micrograph in Figure 7A shows particles with a lamellar-platelet morphology, as well as regions with brittle fragments and agglomerations. This morphology is typical of hydrated calcium silicates, especially tobermorite and C–S–H compound phases (Yang et al., 2023).

The chemical mapping analyses (Figures 7B–G) confirm the heterogeneous distribution of the main elements (Ca, Si, Al, Mg, Na, and Fe). The Ca map (Figure 7B) indicates strong concentration in aggregates (Sun et al., 2022), while that of Si (Figure 7C) shows a more uniform distribution, suggesting the formation of Ca–Si phases rich in C–S–H gel (Yang et al., 2023). The presence of Mg appears in more localized spots and in systems that use FGD ash (Fungaro et al., 2020). Na appears diffuse (Figure 7F), consistent with the high Na_2O content identified by XRF (Liao et al., 2019). This characteristic is also reported in materials obtained from FGD residues, where sodium can be incorporated into the C–S–H compound, forming mixed phases (Fungaro et al., 2020). Fe appears as small spots, a behavior typical of finely dispersed iron oxides or hydroxides (ash residues or impurities) that do not structurally integrate into the C–S–H compound network (Tchio et al., 2024).

Finally, the EDS spectrum (Figure 7H) shows intense peaks of Si, Ca, and O, as well as signals of Al, Mg, Na, and Fe. This result confirms the predominant formation of C–S–

H/tobermorite, with secondary phases containing Al and Fe, comparable to the work of Siauciunas et al. (2021).

Figure 7. SEM/EDS micrographs of the SCF compound synthesized from FGD ash where: morphological mapping (A); elemental mapping (B to H)

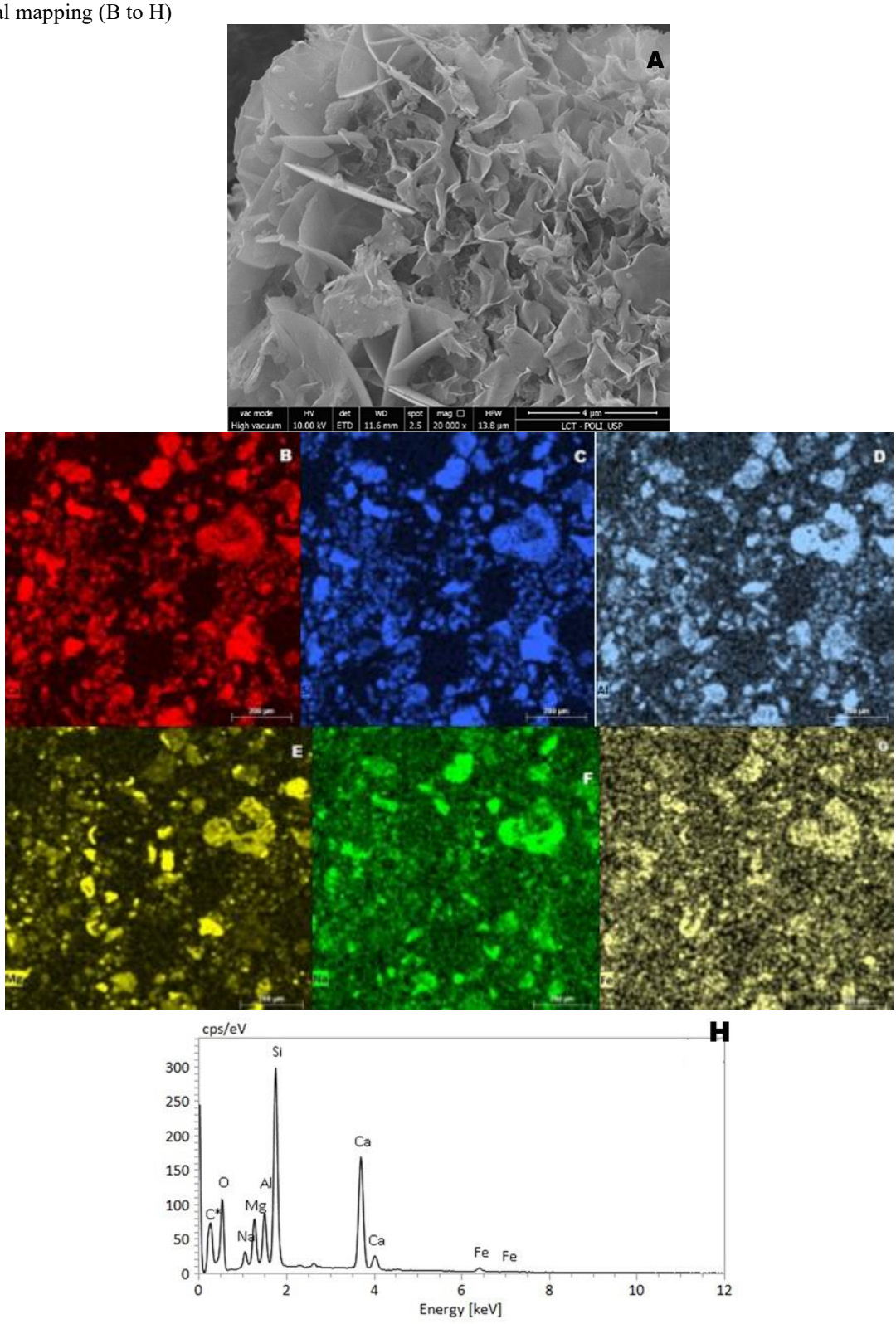

Source: Prepared by the authors

3.2.8 TGA

The evaluation of the thermal stability of C–S–H compounds containing tobermorite is fundamental for understanding the structural transformations and progressive dehydration that occur with increasing temperature, directly affecting their mineralogical composition and functional performance. This parameter allows for the identification of the stages of physically adsorbed and structural water loss, as well as the decomposition of C–S–H phases, providing the basis to correlate thermal changes with the chemical and structural stability of the material (Lothenbach et al., 2011; Houston et al., 2009; Richardson, 2008). Figure 8 shows the graphical behavior of the TGA analysis and its derivative for the SCF compound.

Figure 8. Thermogravimetric (TGA) and derivative (DTG) curves of the SCF compound synthesized from FGD ash

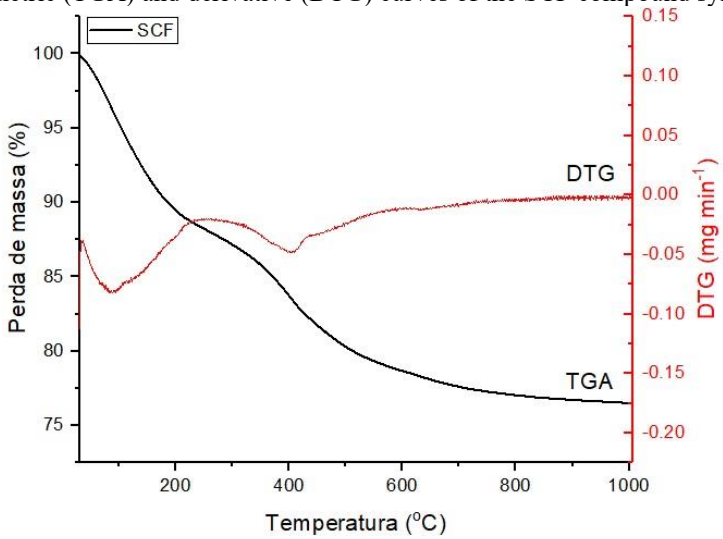

Source: Prepared by the authors

The thermogravimetric analysis (TGA) and its derivative (DTG) of the SCF compound show three distinct regions of mass loss, corresponding to different thermal events related to dehydration and decarbonation of the phases present in the material.

The first stage of mass loss occurs up to approximately 200 °C and is associated with the elimination of physically adsorbed water and interlayer water from the calcium silicate hydrate (C–S–H) phases. This stage is typical of materials containing tobermorite, xonotlite, or amorphous C–S–H, as reported by Li et al. (2020) and Guo and Song (2021), who observed similar behavior in C–S–H compounds synthesized from industrial residues. The mass loss in this range evidences the presence of hydrated species and a microstructure with high surface area, characteristic of hydration products of $CaO–SiO_2$.

The second stage corresponds to the structural dehydration of C–S–H compounds, with the release of coordinated water and partial collapse of the structural layers. This range is related to the

dehydroxylation of Si–OH and Ca–OH groups present in the calcium silicate hydrate matrix. According to WU et al. (2020), in studies with synthetic tobermorite, the main loss in this region occurs between 180 and 450 °C, which confirms the intermediate thermal stability of calcium silicate hydrates formed from FGD residues. The presence of a more defined peak in the DTG curve in this range suggests the predominance of a semicrystalline phase similar to tobermorite.

The third region, which extends from approximately 500 °C to 900–1000 °C, is attributed to the decarbonation of calcium carbonates formed during exposure of the material to atmospheric CO_2, as well as the residual decomposition of C–S–H compound phases into calcium oxide and amorphous silica. The continuous mass loss up to 800 °C indicates the conversion of $CaCO_3$ to CaO, as described by Zhuang et al. (2025) and Yang et al. (2023), who observed similar behavior in CSH-based materials residues rich in Ca and Si.

The sum of mass losses in the three regions indicates that the compound exhibits high thermal stability up to about 450 °C, typical of well-formed C–S–H compounds. The presence of a pronounced decarbonation stage evidences the partial formation of $CaCO_3$ during drying or storage, which is common in Ca^{2+}-rich materials exposed to air. These results confirm the formation of characteristic calcium silicate hydrate phases, compatible with those obtained from the controlled hydration of FGD ash, corroborating the efficiency of the synthesis method employed (Rodriguez et al., 2016; LI et al., 2023).

3.2.9 BET

The textural characterization of the SCF compound was performed by N_2 adsorption/desorption at 77 K, with the results presented in Figure 9 (isotherms), Figure 10 (pore size distribution), and Table 3 (textural properties).

The isotherm (Figure 9) is classified as type IV according to IUPAC, characteristic of mesoporous materials (Thommes et al., 2015). Low adsorption is observed at $P/P_0 < 0.1$, indicating reduced microporosity, followed by a progressive increase in the amount adsorbed and a sharp rise at high relative pressures ($P/P_0 > 0.8$), associated with capillary condensation in mesopores. The hysteresis loop is of type H3, typical of materials formed by lamellar aggregates that produce slit-shaped pores, a behavior frequently observed in C–S–H gels and poorly crystalline tobermorite-like structures (Richardson, 2008).

Figure 9. N_2 adsorption and desorption isotherms at 77 K for the SCF compound (red = adsorption; purple = desorption); and pore size distribution of the SCF compound

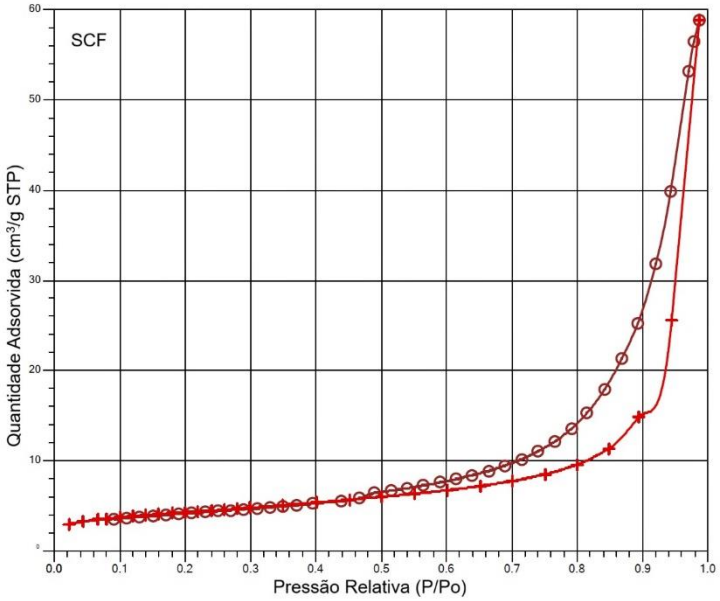

Source: Prepared by the authors

Table 3. Textural properties of the SCF compound

Properties	Value
Specific surface area (m^2/g)	14,85
Mesopore volume (cm^3/g)	0,09
Average mesopore diameter (nm)	21

Source: Prepared by the authors

The textural parameters summarized in Table X show a specific surface area of 14.84 m^2/g, total pore volume of 0.09 cm^3/g, and an average mesopore diameter around 21 nm (≈ 210 Å), values compatible with mesoporous materials in the 2–50 nm range as defined by IUPAC (Thommes et al., 2015). The magnitude of the surface area is directly related to the degree of aggregation of the nanometric units of C–S–H compounds and the presence of interparticle pores.

The pore size distribution (Figure 10), obtained by the BJH method from the desorption branch, shows a predominance of mesopores in the range of 15–30 nm, with a significant absence of micropores (<2 nm) and macropores (>50 nm). The relatively broad peak indicates structural heterogeneity, attributed to the coexistence of intragel and interparticle pores, a common characteristic of C–S–H compounds synthesized by chemical precipitation (Li et al., 2022).

In general, the mesoporous network developed in the SCF compound presents interconnected and accessible pores, a condition favorable for ionic diffusion and potentially suitable for applications in the immobilization of cationic species (Zhang et al., 2020).

Figure 10. Pore size distribution of the SCF compound

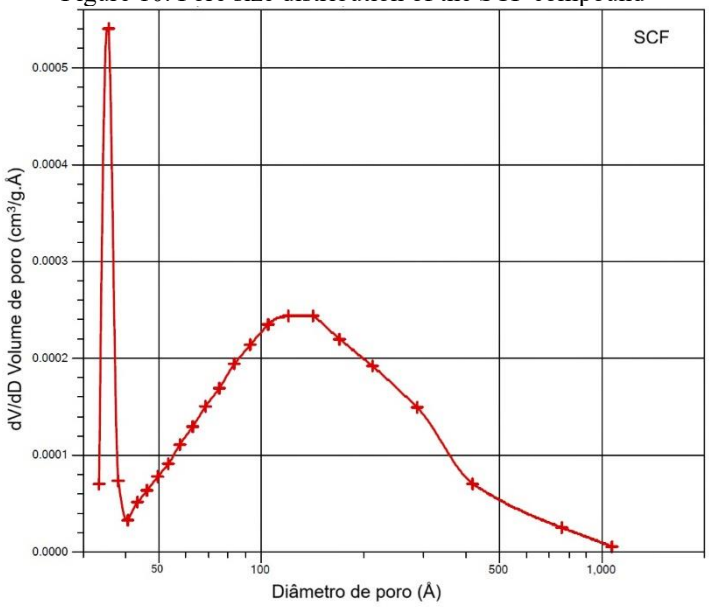

Source: Prepared by the authors

4 CONCLUSION

The bibliometric analysis carried out revealed consistent gaps in the literature related to the correlation between crystalline structure, microstructure, and surface properties of calcium silicate hydrates derived from industrial residues, providing the scientific basis that guided the experimental development of this study.

The SCF compound exhibited composition and structure characteristic of calcium silicate hydrates, with predominant formation of tobermorite and amorphous C–S–H-type phases. The XRF analysis indicated a balanced ratio between CaO and SiO_2, as well as significant incorporation of Na, Al, and Mg, elements that promoted modifications in the silicate network and favored the formation of mixed C–(A,M)–S–H-type phases. The relatively low density (2.10 $g \cdot cm^{-3}$) and polydisperse particle size reflect the porous and partially amorphous nature of the material, consistent with compounds obtained by hydrothermal synthesis from industrial residues.

The XRD, FTIR, and Raman techniques confirmed the presence of crystalline tobermorite associated with semicrystalline C–S–H gels, while electron microscopy revealed a lamellar-platelet morphology and heterogeneous distribution of Ca, Si, Al, Mg, and Na. Thermogravimetric analysis demonstrated high thermal stability up to approximately 450 °C, with typical dehydration and decarbonation behavior of well-developed C–S–H phases. Nitrogen adsorption analysis (BET) indicated a moderate specific surface area (14.85 $m^2 \cdot g^{-1}$) and predominantly mesoporous porosity, consistent with the lamellar aggregates observed by SEM.

The results demonstrated that the adopted synthesis process enabled the formation of a multiphasic, structurally stable compound with textural properties suitable for environmental

applications, particularly for the immobilization of metallic ions and radionuclides in aqueous media. Beyond the technical performance, the use of FGD ash as a raw material directly contributes to circular economy strategies and the valorization of industrial residues, reducing landfill disposal and promoting the reuse of by-products from the energy industry. In this context, the developed material shows potential to contribute to environmental sustainability goals, aligning with the Sustainable Development Goals (SDGs), especially SDG 9 (Industry, Innovation and Infrastructure), 12 (Responsible Consumption and Production), and 13 (Climate Action), reinforcing the scientific and technological relevance of the proposed approach.

AGRADECIMENTOS

The authors would like to thank CNPQ for financial support and the power plant for providing samples of sulfated coal ash.

REFERÊNCIAS

ALCÂNTARA-DOMINGOS, R. R; FUNGARO, D. A. Circular economy: development of calcium silicate hydrated compounds aimed at the sustainable use of waste from the coal industry. **Brazilian Journal of Animal and Environmental Research**, v.8, n.1, p. 1-14, 2025.

ALSHARARI, F. Utilization of industrial, agricultural, and construction waste in cementitious composites: A comprehensive review of their impact on concrete properties and sustainable construction practices. **Materials Today Sustainability**. Volume 29, 101080, March 2025.

ARIA, M.; CUCCURULLO, C. bibliometrix: An R-tool for comprehensive science mapping analysis. **Journal of Informetrics**, v. 11, n. 4, p. 959–975, 2017.

BIAGIONI, C.; MERLINO, S.; BONACCORSI, E. The tobermorite supergroup: a new nomenclature. **Mineralogical Magazine**, Vol. 79(2), pp. 485–495, April 2015.

CHEN, X. *et al*. Preparation of CSHW with flue gas desulfurization gypsum. **Materials**. 15, 2691, 2022.

DIAMOND, S. **Tobermorite and tobermorite-l/ke calcium silicate hydrates: their properties and relationships to clay minerals**. Purdue University- Lafayette, Indiana. August 2, 1963.

DONTHU, N. *et al*. How to conduct a bibliometric analysis: An overview and guidelines. **Journal of Business Research**, v. 133, p. 285–296, 2021.

DURASTANTI, C.; MORETTI, L. Environmental Impacts of Cement Production: A Statistical Analysis. **Appl. Sci**. 10, 8212, 2020.

FERRAZ, D.; PYKA, A. Circular economy, bioeconomy, and sustainable development goals: a systematic literature review. **Environmental Science and Pollution Research**, 30, 37728–37750, 2023.

FUNGARO, D. A.; GROSCH, L. C.; IZIDORO, J. C. Synthesis of Calcium Silicate Hydrate Compounds from Wet Flue Gas Desulfurization (FGD) Waste. **Journal of Applied Materials and Technology**, v. 1, n. 2, p. 88–95, 2020.

GALVÁNKOVÁ, L. *et al*. Tobermorite synthesis under hydrothermal conditions. **Procedia Engineering,** 151, 100 –107, 2016.

GARTNER, E.; MARUYAMA, I.; CHEN, J. A new model for the C-S-H phase formed during the hydration of Portland cements. **Cement and Concrete Research,** 97, 95–106, 2017.

GROSCHE, L. C.; BERTOLINI, T. C. R.; FUNGARO, D. A. Alkaline Hydrothermal Treatment of the Waste Produced in the Semi-Dry Flue Gas Desulfurization System. **International Journal of Advanced Research in Chemical Science**, v. 5, n. 1, p. 9–19, 2018.

GUO, X.; MENG, F.; SHI, H. Microstructure and characterization of hydrothermal synthesis of Al-substituted tobermorite. **Construction and Building Materials**, v. 133, p. 253–260, 2017.

Guo, X.; Song, M. Micro-nanostructures of tobermorite hydrothermal-synthesized from fly ash and municipal solid waste incineration fly ash. **Construction and Building Materials**. 191, 431–439, 2018.

HABERT, G. *et al*. Environmental impacts and decarbonization strategies in the cement and concrete industries. **Nature Reviews Earth & Environment**, v. 1, p. 559–573, 2020.

HOUSTON, J. R. ; MAXWELL, R. S.; CARROLL, S. A. Transformation of meta-stable calcium silicate hydrates to tobermorite: reaction kinetics and molecular structure from XRD and NMR spectroscopy. **Geochemical Transactions,** 10:1, 2009.

HURT, A. P. *et al*. Calcium Silicate Hydrate Cation-Exchanger from Paper Recycling Ash and Waste Container Glass. **Ceramics**, 5, 301–317, 2022.

ISMAIL, M. et al. Decarbonization pathways in medical waste management through circular economy strategies to advance UN-SDGs. **Scientific Reports,** 15:42499, 2025.

JACKSON, M. D. *et al*. Phillipsite and Al-tobermorite mineral cements produced through low-temperature water-rock reactions in Roman marine concrete. **American Mineralogist**, Volume 102, pages 1435–1450, 2017.

JUBB, A. M.; ALLEN, H. C. Vibrational Spectroscopic Characterization of Hematite, Maghemite, and Magnetite Thin Films Produced by Vapor Deposition. **ACS Applied Materials & Interfaces**. VOL. 2, NO. 10, 2804–2812. 2010.

KHALIFA, A. Z. *et al*. Advances in alkali-activation of clay minerals. **Cement and Concrete Research,** 132, 106050, 2020.

KHALILI, F. I. *et al*. Effect of oil shale ash, Al, Zn and H_2O_2 foaming agents on formation of NASH and CSH cementitious gels in alkali activated reactions of kaolin and metakaolin. **Discover Materials,** 5:107, 2015.

KIRKPATRICK, R. J. *et al*. Raman Spectroscopy of C-S-H, Tobermorite, and Jennite. **Advn Cem Bas Mat**. 5: 93-99, 1997.

LALHMUNSIAMA, *et al*. Recent Advances in Adsorption Removal of Cesium from Aquatic Environment. **Appl. Chem. Eng**., Vol. 29, No. 2, 127-137. April 2018.

LI, J. *et al*. Influences of cross-linking and Al incorporation on the intrinsic mechanical properties of tobermorite. **Cement and Concrete Research,** 136, 106170, 2020.

LI, K. *et al*. Effect of microscale C–S–H on the properties of Portland cement and hydration kinetics analysis at different curing temperatures. **Composites Part B**, 280, 111461, 2024.

LI, M. *et al*. Mechanical Properties and Coagulation Characteristics of Flue Gas Desulfurization Gypsum-Based Polymer Materials. **Polymers**, 14, 4761, 2022.

LIAO, W. *et al*. Effect of Different Aluminum Substitution Rates on the Structure of Tobermorite. **Materials**, v.12, n.22, p.3765, 2019.

LIU, H. *et al*. The influence of defects on the mechanical behaviors of tobermorite and C-S-H-A comparative study. **Case Studies in Construction Materials**. Volume 22, e04417, july 2025.

LIU, Q. *et al*. Ultra-purification of heavy metals and robustness of calcium silicate hydrate (C–S–H) nanocomposites. **Chemosphere**, 335, 139063, 2023.

LOTHENBACH, B.; JANSEN, D.; YAN, Y.; SCHREINER, J. Solubility and characterization of synthesized 11 Å Al-tobermorite. **Cement and Concrete Research.** 159, 106871, 2022.

LOTHENBACH, B.; SCRIVENER, K.; HOOTON, R. D. Supplementary cementitious materials. **Cement and Concrete Research**, 41, 1244–1256, 2011.

MADADI, A.; WEI, J. Characterization of Calcium Silicate Hydrate Gels with Different Calcium to Silica Ratios and Polymer Modifications. **Gels**, 8, 75, 2022.

MADDALENA, R. *et al*. Direct synthesis of a solid calcium-silicate-hydrate (C-S-H). **Construction and Building Materials**, v. 223, p. 554–560, 2019.

MALFERRARI, D. *et al*. Al-Substituted Tobermorites: An Effective Cation Exchanger Synthesized from "End-of-Waste" Materials. **ACS Omega**, v.7, n.2, p.1694–1702, 2022.

MATSUI, K. *et al*. *IN SITU* time-resolved x-ray diffraction of tobermorite formation process under hydrothermal condition: Influence of reactive al compound. **Powder Diffraction**, Volume 26, Special Issue 2, pp. 134 – 137, june 2011.

MILAK, P. *et al*. Evaluation of Flue Gas Desulfurization (FGD) Waste Potentiality from Coal-Fired Power Plants to Obtain Alkali-Activated Materials. **Minerals,** 15, 930, 2025.

ORTABOY, S. *et al*. Effects of CO_2 and temperature on the structure and chemistry of C–(A–)S–H investigated by Raman spectroscopy. **RSC Adv.**, 7, 48925, 2017.

PROVIS, J. L. Alkali-activated materials. **Cement and Concrete Research**, v. 114, p. 40–48, 2020.

QUAN, T. N.; CHIEU, L. P. H.; KIEN, P. T. Engineering C–S–H Sorbents via Hydrothermal Synthesis of PV Glass and Carbide Sludge for Chromium (III) Removal. **Coatings**, 15, 733, 2025.

RAHMAN, H.; LI. Q.; COLEMAN, N. J. Waste Glass-Derived Tobermorite Carriers for Ag^{+} and Zn^{2+} Ions. **J. Compos. Sci**., 6, 52, 2022.

RICHARDSON, I. G. The calcium silicate hydrates. **Cement and Concrete Research,** 38, 137–158, 2008.

RITZ, M. Infrared and Raman Spectroscopy of Mullite Ceramics Synthesized from Fly Ash and Kaolin. **Minerals,** 13, 864, 2023.

RODRIGUEZ, C. *et al*. Low-Carbon Autoclaved Alkali-Activated Blast Furnace Slag Concrete: Microstructure and Mechanical Properties. **Appl. Sci**., 16, 1178, 2026.

SCRIVENER, K. L.; JOHN, V. M.; GARTNER, E. M. Eco-efficient cements: Potential economically viable solutions for a low-CO_2 cement-based materials industry. **Cement and Concrete Research,** 114, 2–26, 2018.

SIAUCIUNAS, S.; SMALAKYS, G.; DAMBRAUSKAS, T. Porosity of calcium silicate hydrates synthesized from natural rocks. **Materials**, v. 14, n. 19, p. 5592, 2021.

SUN, S. *et al*. Fly ash derived calcium silicate hydrate as a highly efficient and fast adsorbent for Cu(II) ions: role of copolymer functionalization. **RSC Adv**. 12, 22843, 2022.

TANG, S. *et al*. Structure, fractality, mechanics and durability of Calcium Silicate Hydrates. **Fractal and Fractional**, v. 5, n. 2, p. 47, 2021.

TAYLOR, H. F. W. **Cement Chemistry**. 2nd Edition, Thomas Telford, London. 1997.

TELESCA, A. *et al*. Flue gas desulfurization gypsum and coal fly ash as basic components of prefabricated building materials. **Waste Management,** 33, 628–633, 2023.

TCHIO, J. A. *et al*. Design and characterization of iron–calcium–aluminium–silicate–hydrate as low-temperature Binder. **Innovative Infrastructure Solutions**, 9:42, 2024.

THOMMES, M. *et al*. Physisorption of gases, with special reference to the evaluation of surface area and pore size distribution (IUPAC Technical Report). **Pure Appl. Chem**. 87(9-10): 1051–1069, 2015.

TSVETKOV, M. V. *et al*. Influence of Sodium Oxide on the Fusion of Solid Municipal Waste Ash. **Russian Journal of Physical Chemistry B**, Vol. 14, No. 4, pp. 647–653, 2020.

VAN ECK, N. J.; WALTMAN, L. Software survey: VOSviewer, a computer program for bibliometric mapping. **Scientometrics**, v. 84, p. 523–538, 2010.

VIDMER, A.; SCLAUZERO, G.; PASQUARELLO, A. Infrared spectra of jennite and tobermorite from first-principles. **Cement and Concrete Research**, v. 60, p. 11–23, 2014.

WANG, Z. *et al*. Efficient removal of phosphate and ammonium from water by mesoporous tobermorite prepared from fly ash. **Journal of Environmental Chemical Engineering**, 10, 107400, 2022.

WU, Y. *et al*. Crystallization and phase transition of tobermorite synthesized by hydrothermal reaction from dicalcium silicate. **Int J Appl Ceram Technol**. 17: 1213–1223, 2020.

XU, L. *et al*. Utilization of flue gas desulfurization gypsum for producing calcium sulfoaluminate cement. **Journal of Cleaner Production**, v. 161, p. 803–811, 2017.

YAN, Y. *et al*. Effect of alkali hydroxide on calcium silicate hydrate (C-S-H). **Cementand Concrete Research**. 151, 106636, 2022.

YANG, Z. *et al*. Study on Crystal Growth of Tobermorite Synthesized by Calcium Silicate Slag and Silica Fume. **Materials**. 16, 1288, 2023.

ZHANG, T. *et al*. Cheeseman, C. R. Immobilization of Radionuclide ^{133}Cs by Magnesium Silicate Hydrate Cement. **Materials**, 13, 146, 2020.

ŻAK, R.; DEJA, J. Spectroscopy study of Zn, Cd, Pb and Cr ions immobilization on C-S-H phase. **Spectrochimica Acta Part A: Molecular and Biomolecular Spectroscopy** 134, 614–620, 2015.

ZHAO, Z. *et al*. Synthesis, Characterization and Hexavalent Chromium Adsorption Characteristics of Aluminumand Sucrose-Incorporated Tobermorite. **Materials**, 10, 597, 2017.

ZHU, K. *et al*. Study on synthesis of C–S–H gel and its immobilization of heavy metals. **Crystals**, 14, 864, 2024.

ZHUANG, D.; CHEN, Z.; SUN, B. Thermal Decomposition of Calcium Carbonate at Multiple Heating Rates in Different Atmospheres Using the Techniques of TG, DTG, and DSC. **Crystals**, 15, 108 2025.